Vol 10 No 9, September 2001
1009-1963/2001/10(09)/0790-06
Chinese Physics
© 2001 Chin. Phys. Soc.
and IOP Publishing Ltd

NUMERICAL ANALYSIS OF A CHAOTIC SYSTEM

Ren Zhi-jian(任志坚)†
College of Electrical & Electronic Engineering, Huazhong (Central China) University of Science and Technology, Wuhan 430074, China

(Received 7 August 2000; revised manuscript received 25 April 2001)

This paper further proves that a single spiral strange attractor can be observed in an extremely simple autonomous electrical circuit by computer simulation. It is of third order and has only one nonlinear element: a three-segment piecewise linear resistor. The digital analyses show that the strange attractor has peculiar features compared with other third-order differential systems.

Keywords: nonlinear circuit, strange attractor
PACC: 0545

I. INTRODUCTION

There are two common routes leading to chaos in the third-order differential system: one is period-doubling, and the other is period-adding. Both phenomena can be seen from the simulation of circuits.[1,2] Using a nonlinear circuit to simulate chaos is a common experimental method for chaos research. So far, most research is in the area of the first route to chaos in the nonlinear circuit. Research in the second route to chaos is relatively limited. This paper gives a detailed digital analysis for a chaotic attractor with a single spiral structure which is observed in a circuit via the period-adding route to chaos. This chaotic attractor was observed in an extremely simple autonomous electrical circuit. Extensive experimental measurements of this circuit have been reported earlier.[2] The circuit is of third order and has only one nonlinear element: a three-segment piece-wise linear resistor. The detailed research shows that the characteristics of an equilibrium point will determine the structure of the chaotic attractor and the nonlinearity of the nonlinear element will determine the route of approach to chaos.

II. SYSTEM DESCRIPTION

We consider the circuit of Fig.1, of which the constitutive relation of the nonlinear resistor is given in Fig.2. The system dynamics is described by the differential equations

$$\begin{aligned} C_1 f'(i_R)\frac{\mathrm{d}i_R}{\mathrm{d}t} &= -(G_1+G_2)f(i_R) \\ &\quad - i_R + G_2 v_{C_2} + EG_1, \\ C_2\frac{\mathrm{d}v_{C_2}}{\mathrm{d}t} &= G_2(f(i_R)-v_{C_2}) - i_L, \\ L\frac{\mathrm{d}i_L}{\mathrm{d}t} &= v_{C_2}, \end{aligned} \tag{1}$$

where i_R, v_{C_2} and i_L denote the current through the nonlinear element, the voltage across C_2 and the current through L, respectively, and $f(i_R)$ is the piecewise linear function shown in Fig.2,

$$f(i_R) = a_1 + a_2 i_R + a_3|i_R - a| + a_4|i_R - b|, \tag{2}$$

and

$$f'(i_R) = \begin{cases} k1 & i_R \le a, \\ k2 & a < i_R \le b, \\ k3 & i_R > b, \end{cases} \tag{3}$$

where $k1$, $k2$ and $k3$ are the slopes of the three sections of lines, respectively.

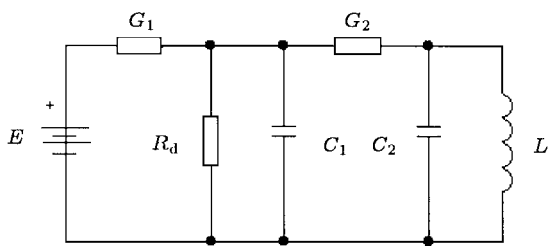


Fig.1. Block diagram of the autonomous circuit which can realize the single spiral attractor.

†Current address: Department of Electronic and Information, Hong Kong Polytechnic University, Hong Kong, China.

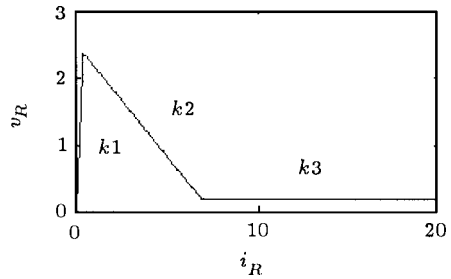


Fig.2. Constitutive relation of the nonlinear resistor.

Ⅲ. DIGITAL ANALYSIS

Figure 3 shows the chaotic attractor observed by solving (1) using the fourth-order Runge–Kutta numerical method with the parameters

$$C_1 = 1.25, C_2 = 0.5, L = 1/24,$$
$$G_1 = 0.8, G_2 = 1.8, E = 7.771,$$
$$k1 = 320, k2 = -0.3346, k3 = 0.002,$$
$$a = 0.0744, b = 6.525, a_1 = 0.0739,$$
$$a_2 = 160.004, a_3 = -160.1673, a_4 = 0.1713. \quad (4)$$

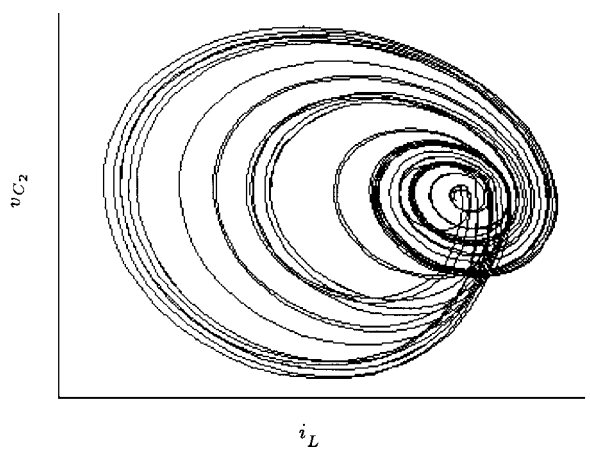


Fig.3. Projection onto the (v_{C_2}, i_L)-plane of the single spiral strange attractor.

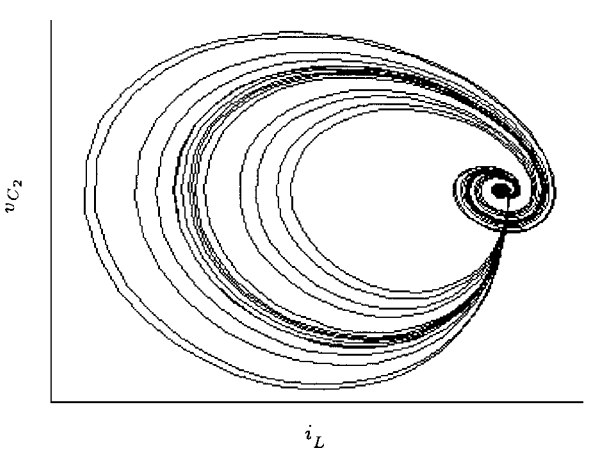


Fig.4. Projection onto the (v_{C_2}, i_L)-plane of the single spiral strange attractor with a convergence centre.

By further changing the parameters of the circuit, for example, G_1 from 0.8 to 1, G_2 from 1.8 to 2.4, a chaotic attractor with a convergence centre is observed, as shown in Fig.4. These simulation results of the attractor are the same as the experimental results given in Ref.[2]. Figure 5 shows the power spectra for the time waveforms of the three state variables v_{C_1}, v_{C_2} and i_L. The continuous spectra indicate that the single spiral attractor is a chaotic attractor. The power spectra for v_{C_1} and i_L have notable low-frequency components while the power spectrum for v_{C_2} does not. We will see in the next section that this stems from the fact that the v_{C_2}-component of the equilibrium point is zero while the v_{C_1}-component and the i_L-component are non-zero. Therefore, the

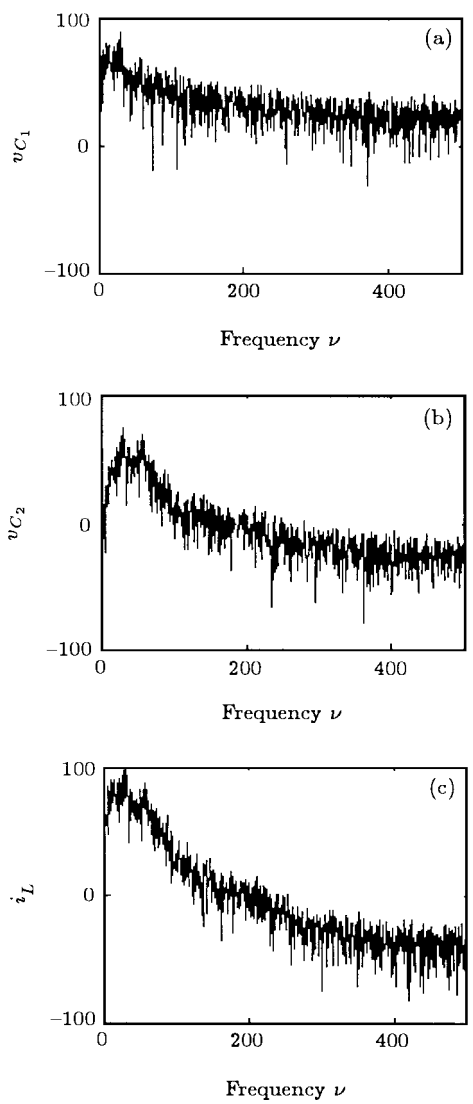


Fig.5. Power spectra of time waveform associated with the three state variables: (a) v_{C_1}; (b) v_{C_2}; (c) i_L. Vertical scale: 100 dB/division. Horizontal axis: normalized frequency.

oscillations of v_{C_2} have essentially no "dc" bias while the oscillations of v_{C_1} and i_L are biased. Figure 6 shows a Poincaré section at v_{C_1}=2.1, in which all points are distributed along an arc.

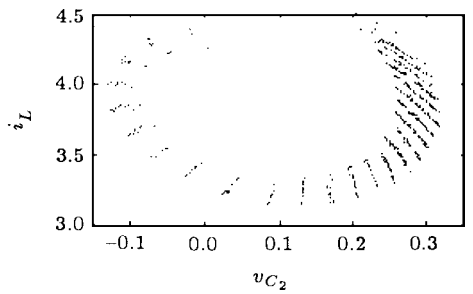


Fig.6. The Poincaré section.

IV. ANALYSIS OF THE STRUCTURE OF THE ATTRACTOR

Putting equations (1) equal to zero, the equilibrium point can be solved. There is only one equilibrium point P:

$$P = (v_{C_{1e}}, v_{C_{2e}}, i_{Re}) = (2.3306, 0, 4.195)$$

with associated parameters given in (4). The equilibrium point has one real eigenvalue and two complex conjugate eigenvalues. The real eigenvalue associated parameters given in (4) is

$$\lambda_1 \approx 0.3473,$$

and the others are

$$\lambda_{2,3} \approx -1.8182 \pm \mathrm{j}6.2971.$$

The eigenvector corresponding to the positive real eigenvalue is

$$V_1 \approx (-0.8629, 0.0073, 0.5053).$$

Replacing i_R with v_{C_1}, the eigenvector V_1 is replaced by

$$v_1 \approx (-276.1309, 0.0073, 0.5053).$$

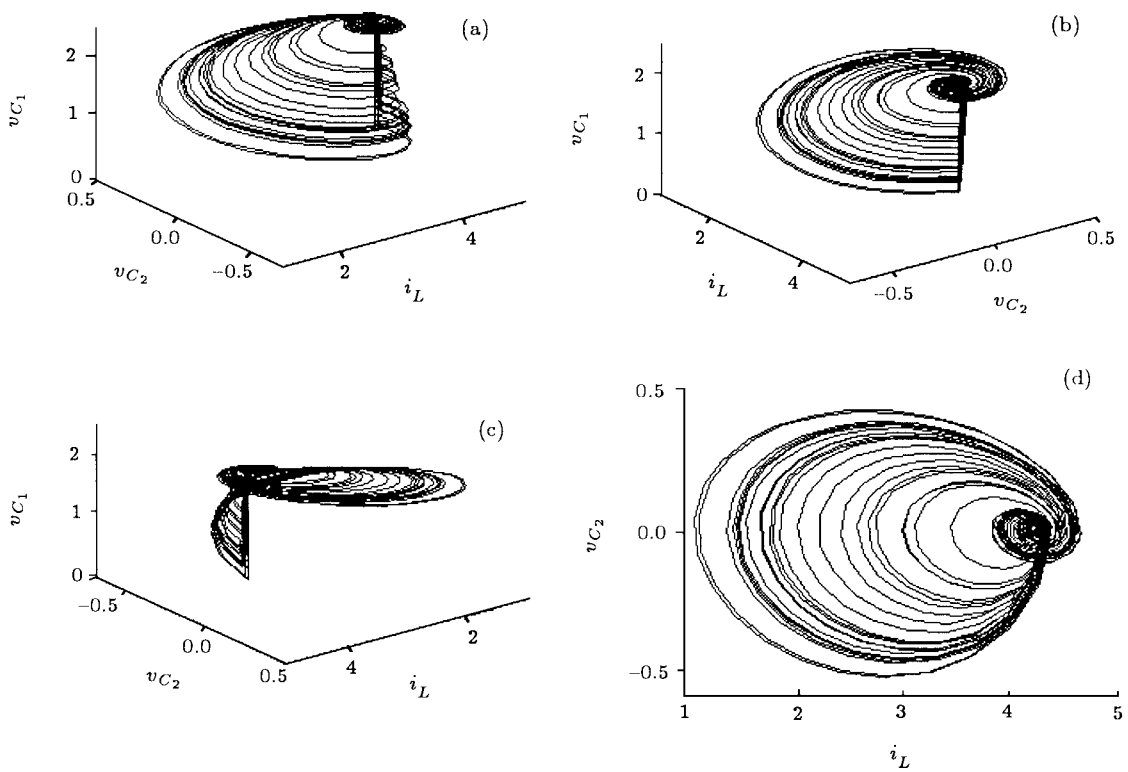


Fig.7. Three-dimensional diagram of the single spiral strange attractor viewed from four angles: (a) viewed at the azimuth –37.5° and the elevation 35°; (b) viewed at the azimuth 52.5° and the elevation 35°; (c) viewed at the azimuth 142.5° and the elevation 35°; (d) viewed at the azimuth 0° and the elevation 90°.

The positive real eigenvalue means that P is unstable. The orbit $e^{0.3473}v_1$ near P will radiate from P along v_1. The orbit corresponding to $\lambda_{2,3}$ will converge at P and form a spiral orbit because the real part of the complex conjugate eigenvalue is negative. Due to their mutual effect on each other, the phase orbit near P has a single spiral chaotic attractor (SSCA) structure with a convergence centre. Figure 7 shows in detail the attractor at different viewing angles. The view of the attractor from right side at the azimuth –37.5° and the elevation 35° is shown in Fig.7(a). Figure 7(b) shows the attractor at the azimuth rotated to 53.5°. Figure 7(c) displays the back of the attractor in Fig.7(a). We also view the attractor from the vertical direction in Fig.7(d). From Fig.7, we may observe that the phase orbit far from P spirals in the direction of the equilibrium point little by little at first. When it draws near to the equilibrium point, it will suddenly and rapidly turn away from the equilibrium point.

V. COMPARISON WITH OTHER CHAOTIC ATTRACTORS

A. Structure of attractor

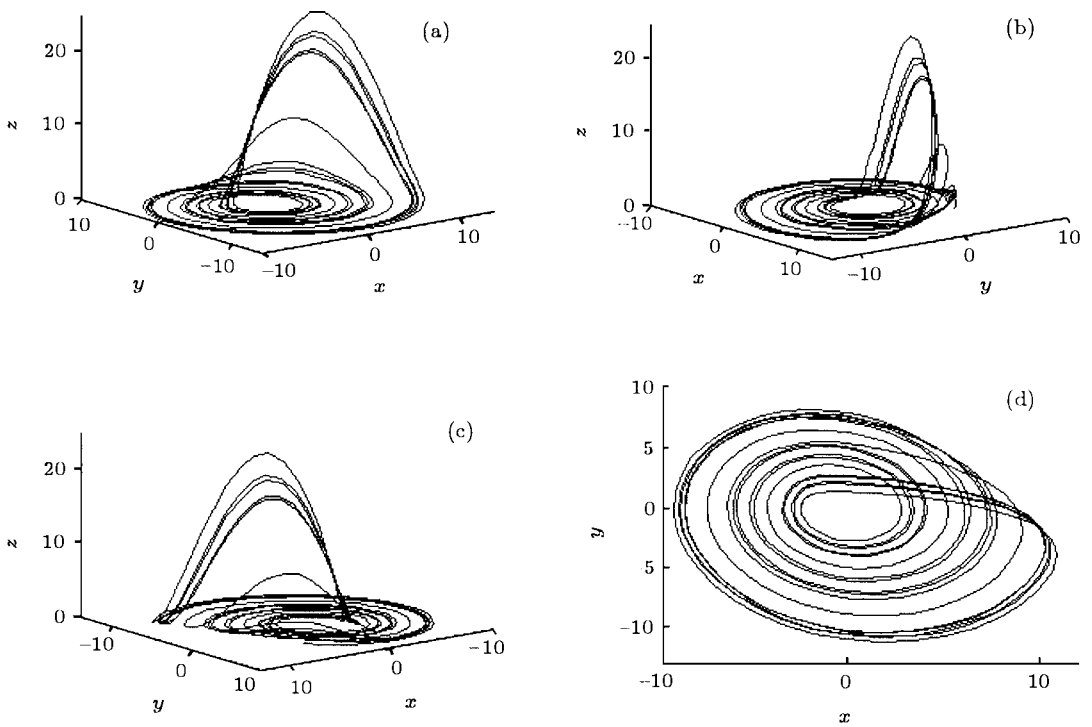


Fig.8. Three-dimensional diagram of the Rössler attactor viewed from four angles: (a) viewed at the azimuth –37.5° and the elevation 20°; (b) viewed at the azimuth 52.5° and the elevation 20°; (c) viewed at the azimuth 142.5° and the elevation 20°; (d) viewed at the azimuth 0° and the elevation 90°.

Compared with other chaotic attractors observed in the third-order differential system, for example, the Lorenz attractor,[3] Rössler attractor[4] and the double scroll observed from Chua's circuit,[1] the SSCA is entirely different. The first difference is the sign of the eigenvalue of the equilibrium point. The positive eigenvalue of the SSCA is a part of the pure real eigenvalue while the positive eigenvalue of the other chaotic attractors mentioned above are a part of the two complex conjugate eigenvalues. This results in the difference in the structure of the attractor. The SSCA has a convergence centre while the others do not. Let us take the Rössler attractor as an example of comparison. Figure 8 shows the detail of the Rössler attractor at four viewing angles: Fig.8(a) is the view of the right side; Fig.8(b) is the view rotated to 90°; Fig.8(c) is the view of the back of the attractor in Fig.8(a); and Fig.8(d) is the projection of the attractor onto the x-y plane.

From Fig.8, we can see that no convergence centre

exists in the attractor. The reason can be found from eigenvalue analysis. The Rössler attractor has a negative real eigenvalue corresponding to the equilibrium point

$$\lambda_1 \approx -5.6870,$$

and a pair of complex conjugate eigenvalues with a positive real part

$$\lambda_{2,3} \approx 0.0970 \pm \mathrm{j}0.9952,$$

associated with the bifurcation parameter c=5.7. The eigenvector corresponding to the negative real eigenvalue is

$$V_1 \approx (0.1682, -0.0286, 0.9853).$$

The complex conjugate eigenvalues with a positive sign determine that the orbit of the attractor near the equilibrium point turns from inside outward. Then it turns along the V_1 direction to the equilibrium point. When it is close to the equilibrium point, it turns from inside outward again. Then it repeats itself ceaselessly.

The Lorenz attractor and the double scroll have two symmetric equilibrium points besides the origin. The two equilibrium points have a negative real eigenvalue and a pair of complex conjugate eigenvalues, also with positive real parts. Therefore, their trajectories of attractors, like the Rössler attractor, turn from inside outward but also jump from one equilibrium point to another, then do so repeatedly and ceaselessly.

B. Lyapunov exponents and Lyapunov dimension

In the investigation of low dimensions of dynamic systems, Lyapunov exponents represent the sensitivity that chaotic orbits depend on the initial values. It shows the stability of the dynamic system.[5−8] Compared with the Rössler attractor, this chaotic attractor has a significantly larger positive Lyapunov exponent of about 0.092, while that of the Rössler attractor is 0.09.[7] It shows that the expansion rate of this attractor is somewhat larger than that of the Rössler attractor.

Besides Lyapunov exponents, the Lyapunov dimension is also an important parameter which describes the complexity of a dynamic system. The Lyapunov dimension of the SSCA is about 2.035 while that of the Rössler attractor is 2.01 and that of the double scroll is 2.13.[1] This shows that the SSCA is slightly "thicker" than the Rössler attractor but "thinner" than the double scroll.

C. Route to chaos

The third difference between the SSCA and other chaotic attractors mentioned above is the route to chaos. The route to chaos of SSCA is via period-adding,[2] while that of the others is via period-doubling.[1,3,4] One should note that the network structure shown in Fig.1 is the same as Chua's circuit which gives rise to the double scroll chaotic attractor.[1] The only difference between them is that they have entirely different nonlinear elements. The nonlinear element in Fig.2 is a type of current-control element and its characteristic is not symmetric, while that in Chua's circuit is a type of voltage-control element with symmetric characteristics. It has been shown that the same nonlinear element of Fig.2, when used in second-order non-autonomous circuits, also gives rise to chaotic phenomena via period-adding.[9,10] The comparison of these experiments shows that it is the nonlinear element that determines the route to chaos,[2,9] and, obviously, this type of nonlinear element generally leads to a period-adding route to chaos.

VI. CONCLUSION

The analyses above indicate that the SSCA has an individual character compared with other chaotic attractors observed from the same third-order differential system. There are two main differences between them. Firstly, the part of positive eigenvalues is different. The former has a positive pure real eigenvalue and a pair of complex eigenvalues with negative real parts while the latter has a negative pure real eigenvalue and a pair of complex eigenvalues with positive real parts, corresponding to each equilibrium point besides the origin. The positive eigenvalue means that the equilibrium point is unstable. For the SSCA, the phase orbit near the equilibrium point radiates from the equilibrium point along the direction of the eigenvector corresponding to the positive real eigenvalue. Because of the effect of the complex eigenvalues with negative real parts, the phase orbit will turn from outside inward and converge to the equilibrium point. When it is close to the equilibrium point, it will repeat the process above. This shows that the equilibrium point has an unstable node and a stable focus so that the single spiral attractor structure has a convergent centre. The other chaotic attractors mentioned

above have a negative pure real eigenvalue. The positive eigenvalues are complex conjugates. This will make each equilibrium point besides the origin have a stable node and an unstable focus so that the phase orbit near the equilibrium points will turn from inside outward. It will not converge at the equilibrium point.

Another difference is the route to chaos. The route to chaos of the SSCA is period-adding while that of the others is period-doubling. This is due to the different nonlinear characteristics. The nonlinear characteristics of a type of current-control element will result in a route to chaos via period-adding. The nonlinear characteristics of a type of voltage-control element will result in a route to chaos via period-doubling. Therefore, the characteristics of the equilibrium point determine the structure of chaotic attractor, and the nonlinearity of the nonlinear element determines the route to chaos.

References

[1] Matsumoto T, Chua L O and Komuro M 1985 *IEEE Trans. Circuits Syst.* **32** 797

[2] Ren Z J and Zhang J R 1995 *Acta Phys. Sin.* **44** 345 (in Chinese)

[3] Lorenz E N 1963 *J. Atmos. Sci.* **20** 130

[4] Rössler O E 1976 *Phys. Lett.* **57A** 397

[5] Yuan J and Xiao X C 1997 *Acta Phys. Sin.* **46** 1300 (in Chinese)

[6] Ma W Q *et al* 1999 *Acta Phys. Sin.* **48** 787 (in Chinese)

[7] Yang S Q *et al* 2000 *Acta Phys. Sin.* **49** 636 (in Chinese)

[8] Ke X Z and Wu Z S 1998 *Acta Phys. Sin.* **47** 1436 (in Chinese)

[9] Chua L O, Yao Y and Yang Q 1986 *Int. J. Circuit Theory Appl.* **14** 315

[10] Kennedy M P and Chua L O 1986 *IEEE Trans. Circuits Syst.* **33** 974